TOWARDS TEMPORAL INFERENCE FOR SHAPE RECOGNITION FROM WHISKERS

Charles Fox, Mat Evans and Tony Prescott
Adaptive Behavior Research Group
University of Sheffield

ABSTRACT

Previous work on shape recognition from whisker-like sensors has taken two approaches. First, static analysis from beam theory has been used to estimate contact points. Second, dynamic analysis has estimated contact points by considering vibrations set up on contact. This paper proposes additional methods which utilize full time-series data from whiskers. Full generative models may be intractable but approximated by discriminative classifiers. Early results show that object location and velocity may be discriminated simultaneously.

I. INTRODUCTION

The recognition of shape is an useful sub-task of robot navigation and other cognitive tasks. For example, commercial robot vacuum cleaners navigate using point collisions only (e.g. [1]) and could be improved by locating classes of objects in space rather than identical-looking points. The use of tactile whisker sensors for mobile robots has been explored by several authors [2], [3], [4], [5] and has advantages of functioning in foggy environments and of being covert.

The mechanics of whisker behavior are described by the theory of beams, as used in Civil Engineering [6] and briefly reviewed below. On making contact with an external object, whiskers bend, giving rise to measurable curvature at their bases. Whiskers also vibrate when they are stuck by object contact, as described by the theory of mechanical vibration analysis [7]. Static and dynamic analysis of beams are often considered as different fields of Engineering, and this divide has continued into whisker sensor research, yielding two distinct methods for shape detection based on the two theories.

This paper reviews static and dynamic whisker analysis then considers forward simulation models of whiskers and inverse models for obtaining single contact points from whisker sensors. It describes new generative and discriminative time-series approaches which may be capable of making inferences about shapes and motion rather than single points, and gives results from a preliminary discriminative implementation.

II. WHISKER MECHANICS

II-A. Static analysis

The beam theorem of Euler and Bernoulli. For a *pure* bending moment (i.e. pairs of forces M at the ends of the beam which rotate as the beam bends, and the center of mass pinned), a small segment of a beam of Young's modulus E and cross-sectional moment of inertia I bends circularly about a center of curvature at radius R, with

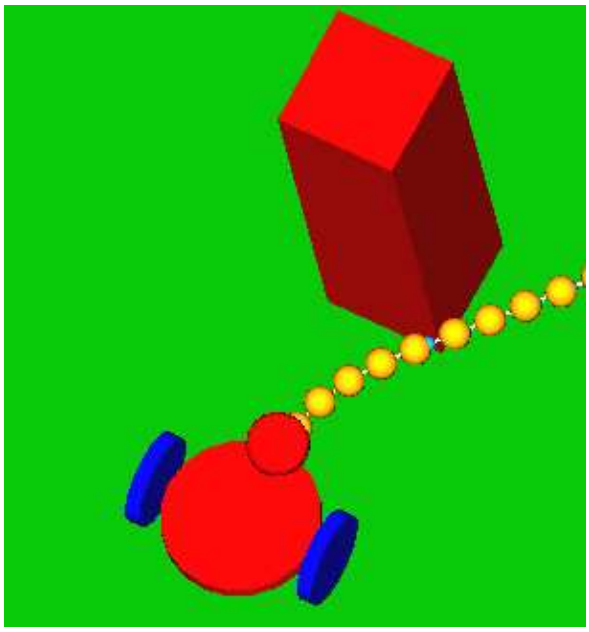

Figure 1. Physical simulation of whiskered robot.

$$\frac{1}{R} = \frac{M}{EI}.$$

(A standard proof is given in the appendix). For example, one of the bending pair could be a contact force when a whisker is bent by an external object; the other bending force and the pin are provided by the base of the whisker. The *area* moment of inertia $I = I(x)$ is that of the cross-sectional *disc*, about the neutral axis. For homogeneous non-tapered whiskers it is constant along x but in general it could be a function of x.

Rather than work with radii of curvature, it is often useful to work with spatial derivatives. By geometry alone, we have for a circle of radius R,

$$\frac{1}{R} = \frac{d^2v/dx^2}{(1 + (dv/dx)^2)^{3/2}}$$

where v is orthogonal axis to x in the whisker's bending

plane. For small deflections dv/dx this reduces to

$$\frac{1}{R} \approx \frac{d^2v}{dx^2}.$$

The *Double integration method* may be used to find the shape of a bending whisker if we are given the moments applied at each point along it. (There is usually a single contact point, which excerpts a variable but effectively unlimited force to oppose the whisker pushing into it. Whiskers are small compared to most external objects so we ignore the effect of the opposite force acting on the object.)

$$v(x) = \int \int \frac{M(x)}{E(x)I} dx^2 + c_0$$

The constant c_0 is set by the boundary condition that the whisker base is fixed in a known position.

Whiskers typically make contact with objects at a single point only, due to their curvature. If a contact force W is applied at distance C from the whisker base then the moment experienced at each point x along the whisker is

$$M(x) = \{ \begin{array}{ll} W(C-x) & : x < C \\ 0 & : x \geq C \end{array}$$

Inserting this moment form into the double integration equation shows that the whisker bends cubically up to the contact point, and is linear afterwards:

$$\frac{EI}{W} v(x) = \begin{array}{ll} \frac{1}{2}Cx^2 - \frac{1}{6}x^3 & : x < C \\ \frac{1}{2}C^2x - \frac{1}{6}C^3 & : x \geq C \end{array}$$

The $x < C$ condition describes the shape from the base of the beam to the contact, and a small part of this region close to the base is typically observable by sensors. The cubic equation has two unknowns, W and C, so requires two observations to solve. These could be observations of the position $v(x)$ at two points, or its gradient and curvature,

$$\frac{dv}{dx} = \frac{W}{EI}(Cx - \frac{1}{2}x^2)$$
$$\frac{d^2v}{dx^2} = \frac{W}{EI}(C - x)$$

or other variables from which any of the above may be derived. Note that the position and gradient (but not curvature) are always zero at the base itself, so are not useful measurements. Kaneko [2] used base torque and an angle moved between first contact with an object and at its final location as such a measurement pair. Similarly, Birdwell et al. [3] use the base angle and torque; or alternatively the first temporal derivatives of the same.

If a series of two-variable data points are received, and it is assumed that the whisker is static at each, then a collection of contact points may be located, and used as the basis for shape recognition. In addition, each contact point also contains the information that there is no object in any of the space swept out by the whisker before reaching its static cubic spline. In particular this is useful for distinguishing smooth curved surfaces from sharp edges, as discussed by [4] and [5].

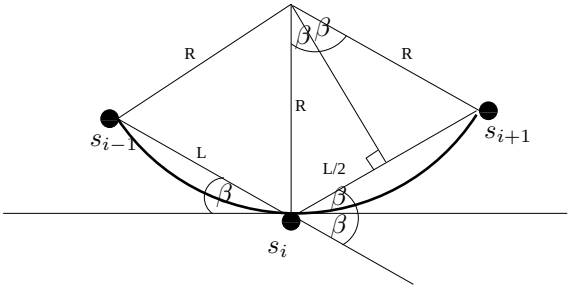

Figure 2. Construction used to derive spring-mass model from the beam theorem.

In practice, for real-world whisking speeds, the whisker is not static at each point, but carries kinetic energy which affects its trajectory. One approach to shape recognition is to estimate the noise level in sensor measurements from their equilibrium values introduced by these deviations from equilibria. The estimates of the contact point coordinates $(C, v(C))$ may then be computed together with error bounds propagated from the sensor uncertainties. There appears, qualitatively, to be a trade-off between speed of whisking (and thus the number of contact points gathered) and the accuracy of the points due to kinetic effects: a whisker driven infinitely slowly would be perfectly accurate. However this approach appears to be throwing away information, as we may have good models of the whisker dynamics and thus be able to account for the 'noise' in terms of the actual dynamic state of the whisker over time.

II-B. Dynamic analysis

Some previous work has considered the use of *simple* dynamic models. Kaneko [8] analyzed a massless beam with a large mass at the tip. When such a beam strikes a contact point, it oscillates in two distinct phases. First – with the beam in contact – the region from the contact point to the tip oscillates with fundamental frequency

$$\omega(C) = \sqrt{\frac{k(C)}{M}} = \sqrt{\frac{12EI}{ML^3(4 - C(3-C)^2)}}$$

where k is the effective spring constant. In the second phase, the beam is not in contact, and oscillates at the natural frequencies of the whole beam. Transitions between the phases may be observed in the base torque, and the contact location deduced from them, under the important assumption that all motion is at stable natural frequencies. Kaneko [8] then proceeded to a non-massless beam, deriving similar equations to estimate C.

In particular this method assumes that there are no transient components due to the initial contact. A low-pass filter was used by Kaneko to remove this 'noise' – which may in fact contain useful information. As with the previous static methods, there is no notion of uncertainty in the estimate. Beams without large masses at the tip often produce ambiguous, bi-valued estimator functions, and the wave equation used in the analysis assumes only

small displacements, which are not valid for large deflections as often experienced by real whiskers. The method must also wait for a complete cycle of both phases to begin making estimates. As with static methods, it is unable to handle moving objects.

Non-generative dynamic models have searched for empirically useful features in the frequency domain of strain signals to predict contact surface properties, usually with regard to classifying texture rather than contact location. In the texture case, it has been noted [9] that the 'ringing' transients produced as the whisker makes and leaves contact with the surface contain useful information. This is the same part of the whisk signal discarded as 'noise' by Kaneko.

III. LIMITATIONS OF CURRENT MODELS

We have reviewed various methods for gaining information about contact location. Static analysis assumes that each data point is at static equilibrium, and discards dynamic effects as noise. State-of-the-art dynamic analysis assumes that all oscillations are at stable natural frequencies, and discards transients as noise; it also only makes use of one sensor. Heuristic classifier-based approaches have found information in transients but do not fuse it with all other available information. All previous methods make point estimates only, not handling uncertainties in various sensors or allowing the possibility to fuse information from multiple sensors. No previous approach has handled moving targets. Other dynamic effects ignored by previous approaches include surface properties such as collision elasticity and surface friction. We thus propose a class of generative time series models capable of accounting for all these effects. We will outline the form of these models, then consider computational inferential and discriminative approximations.

IV. FORWARD SIMULATION

We have constructed a simulation model of a whisker as a series of masses on rotational springs, based on the Open Dynamics Engine (ODE; `www.ode.org`), as shown in fig. 1. Such systems consist of more than two bodies so lack analytic solutions. The number of segments, N, is an important parameter as it controls the complexity of the simulation (and later, of inference) and affects the spring parameters used. Spring constants can be derived as follows. Consider approximating the curved beam with a series of length L segments $\{s_i\}_{i=1}^{N}$ as in fig. 2. The continuous curvature at segment s_i is now replaced by deflection angle $\theta_{i,i+1} = 2\beta$ at each segment. (We write $\theta_{0,1}$ for the angle between the whisker base on the robot and the first segment.) By geometry:

$$R \sin \beta = \frac{L}{2}$$

for small β:

$$R\beta = \frac{L}{2}$$

$$R = \frac{L}{\theta_{i,i+1}}$$

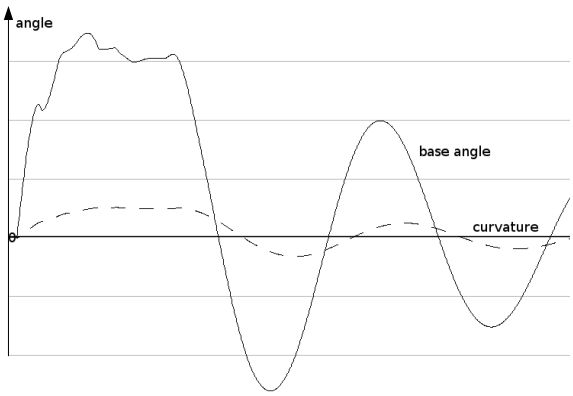

Figure 3. Base angle $\theta_{0,1}$ (solid) and curvature $\theta_{1,2}$ (dashed) during contact with a moving object.

Substitute in from the beam theorem:

$$M = \frac{EI}{L}\theta_{i,i+1}$$

This is now in the form of a rotational spring equation, with

$$k = \frac{EI}{L}$$

The springs also have damping coefficient γ. This may be set using the *Q-value* of an isolated segment, which for light damping is the number of oscillations performed during each loss of $1/e$ of the oscillator energy:

$$Q = \frac{m}{\gamma}\sqrt{\frac{k}{m} - \frac{\gamma^2}{4m^2}}$$

When Q is zero or imaginary the system is critically or heavily damped and no oscillations occur. For light damping (small γ):

$$Q \approx \sqrt{m}\frac{\sqrt{k}}{\gamma}$$

The segment Q-value could be computed analytically from beam theory, measured empirically from a real whisker segment of length L, or – for simulations – simply prescribed. In particular its is often useful to prescribe critical damping.

Collision detection is handled by ODE, as are constraint forces to hold joints together. However we have found that such whisker systems are extremely sensitive to numerical errors and require small time steps to simulate correctly, and we note empirically that there appears to be a monotonic relationship between the joint Q-value and the number of steps per simulation second to avoid error; and between the number of whisker segments and the steps per simulated second. The problem can be reduced to some extend by introducing linear spring elements alternating with the rotational springs. This reduces the magnitude of the required Lagrangian constraint satisfaction forces which are the principal cause of numerical instability. We are considering the design

of a custom ODE joint which combines rotational and linear springs to reduce error further.

The simulation allows us to record sensor-like observations, for example of base angle $\theta_{0,1}$ and base curvature, approximated by $\theta_{1,2}$. It also allows for small random noise forces to be applied at all segments, as would be experienced due to wind and self-motion of the robot body.

Figs. 4 and 3 shows the screen-shots and simulated base angle and curvature for a passive whisker being stuck by a *moving* square object, whose motion is perpendicular to the line of the whisker. The first oscillation includes the contact period; the others occur after the object has passed by the whisker. The shape, contact location and motion of the object affect the time series during the contact period and the subsequent oscillations. (Real whiskers have a much lower Q than simulated here; however this requires much longer computation time to simulate as discussed above, so for development purposes a low Q is used.) Note in particular that in step 5 of fig. 4 the whisker has received large momentum from the object and continuous to move away from it, before springing back to make contact a second time in step 6.

V. INVERSE TIME-SERIES INFERENCE

Fig. 5 shows a slice of a dynamic Bayesian network model for the whisker system. It consists of segment states s_i which each comprise current position and velocity; contact object state c which also comprises position and velocity along with other object properties such as shape, rotation, surface elasticity and friction. The observed base angle $\theta_{0,1}$ and curvature $\theta_{1,2}$, and small noise nodes representing additional forces applied to the segments and contact object. Two time slices are shown horizontally; in reality the model consists of many such slices over the simulation time. The transition relation for the contact object is such as to update its position according to its previous velocity; and allow for changes in velocity according to some prior, as well as any noise forces acting on it. The transition relations for the segments are complex as they include constraint satisfaction forces, but may be modeled implicitly by ODE physics simulation steps. Similarly the observations are obtainable from such simulations.

Drawing samples from the model is simple, and effectively amounts just to running the ODE physics simulation, with appropriate random noises added. A much more challenging task is to infer the most probable explanation of given observed time series. Exact inference is clearly intractable due to the loopiness, continuous-valued nodes, and highly non-linear transitions. However approximate inference by tracking of hypothesis subsets (i.e. particle filtering) [10] may be possible. The whisker domain is especially interesting as the number of segments in the model may be varied, trading off physical accuracy for the number of variables (and hence dimensions) represented in each particle. After drawing random noises, the transition steps can be performed deterministically by calling out to the ODE physics engine to simulate the evolution of each particle.

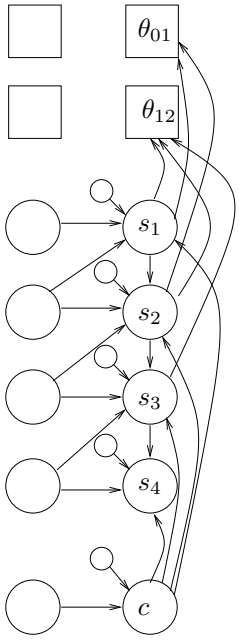

Figure 5. Dynamic Bayesian network slice for the physical whisker model. Small nodes are noise sources; square nodes are observations.

VI. DISCRIMINATIVE APPROXIMATION

We have shown how to set up inference from whiskers as a dynamic Bayesian network based on physical simulation, and suggested that approximate particle filtering inference may be useful. However it is an open question whether any such inference is feasible in real-time. An alternative approach is to construct and train discriminative functions – such as neural networks – mapping directly but approximately from the time-series data to the object state. As well as potentially replacing full inference models, such discriminative methods may be useful as heuristics within them: for example by suggesting new hypotheses to 'inject' into particle filters [11].

VI-A. Template-based discrimination

To demonstrate that at least some useful information is quickly obtainable from the time series by discriminative methods, we here present baseline results for estimating the contact distance d to a moving object using the curvature, $\theta_{12}(t)$, series only. The object is the square box moving at a vertical, fixed velocity as shown in fig. 4. The only variable is the horizontal distance of the box from the whisker base.

Fig. 6 shows examples of curvature series for three contact distances. (Time is unit-less but steps may be though of as milliseconds.) The series make reasonably smooth shape transitions as the contact distance varies. Series were obtained for distances of 1.5cm to 3.0cm, in 1mm steps. (Contacts closer than 1.5cm are difficult to simulate and were discarded.) The first, last and

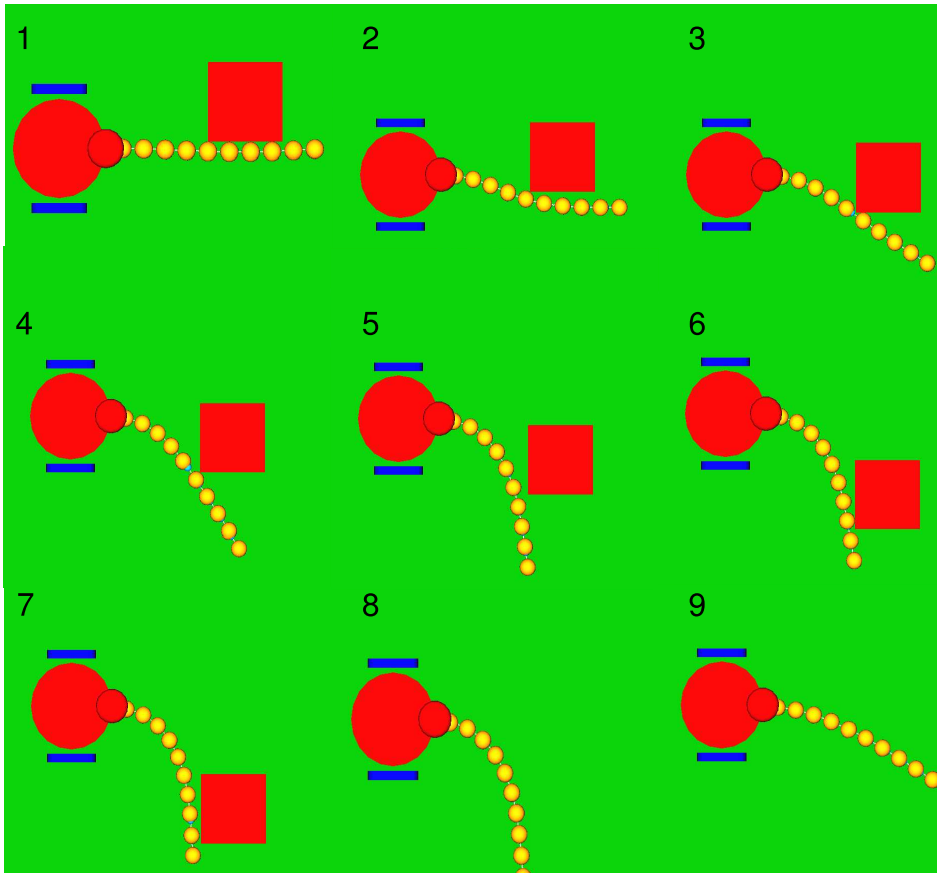

Figure 4. Screen-shots during contact with a moving object. The whisker length is 3cm.

central (2.3cm) points were used as template models. The remaining points' contact distances were then estimated as follows. Define the responsibility $\lambda_o(i)$ of template $m_i(t)$ for an observed series $o(t)$ as the Gaussian

$$\lambda_o(i) = \frac{1}{Z} \exp - \frac{\sum_t (m_i(t) - o(t))^2}{2\sigma^2}$$

where a (unit-less) variance of 5 was chosen by hand as a useful value and Z normalizes the responsibilities over i. Responsibilities for the observed contact distances are shown in fig. 7. Taking the average of the template models' contact distances – weighted by the responsibilities – as an estimate of contact distance, gives the model estimates shown in fig. 8, which have a mean error of 1.2mm.

In a second experiment, both the contact distance and the object vertical velocity were varied together. Nine templates were used, at combinations of minimum, medium and maximum of the two variables, and the same methods as above was applied to estimate both parameters simultaneously. The estimated contact distances *across all velocities* are shown in fig. 9 and the estimated velocities *across all contact distances* are shown in fig. 10.

This is the first published result to our knowledge on simultaneous contact distance and object velocity

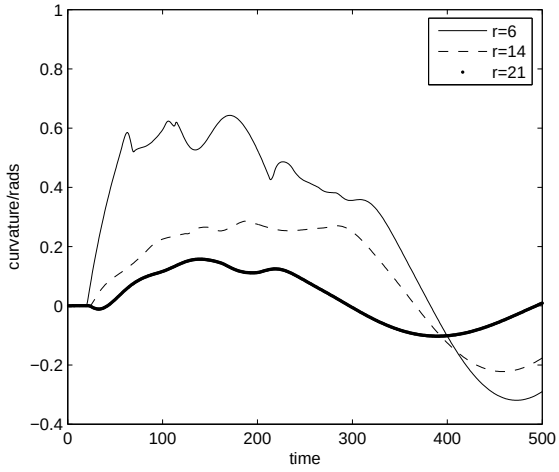

Figure 6. Strain series for three contact distances.

estimation – all previous methods have considered static objects only. It is intended as a proof of concept to show that useful information is contained in whisker time series. However the degradation of accuracy using the simple template method when a second variable is included suggests that this simple method may not

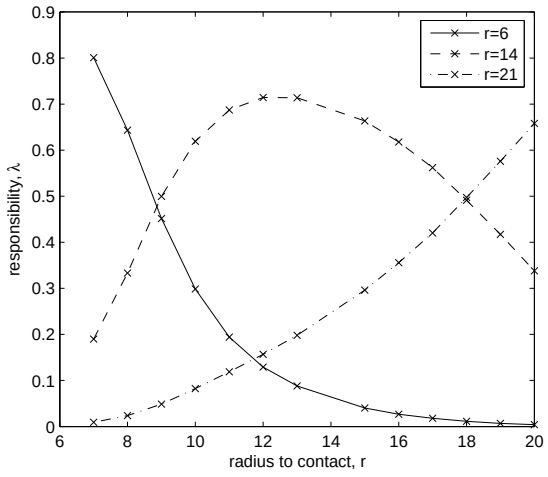

Figure 7. Responsibilities of the three template models for observations at various contact distances (in cm).

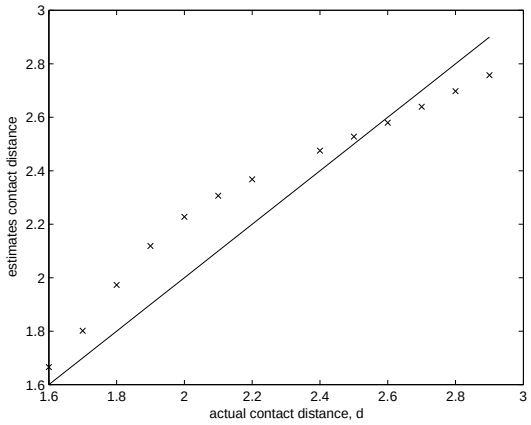

Figure 8. Model contact distance estimates (crosses) against actual contact distances (line), in cm. The mean error is 1.2mm.

generalize to large numbers of object parameters, and hence more detailed models should be more useful.

VII. DISCUSSION

To build and test both generative and discriminative models, it is useful to work with a series of tasks of increasing difficulty. In this case, difficulty mostly corresponds to the size of the parameter space. In addition to reducing the number of segments used in the generative model, the dimension of the contact object may be restricted. A simple scenario is to assume that the only type of object in the world is a frictionless, perfectly elastic plane, moving towards the whisker at known constant velocity. Such an object has only three dimensions: initial shortest distance from the whisker base and rotation. Alternatively, the object could be stationary and the whisker moving *rotationally* into it. Simple shapes such as squares and circles are a little harder, having extra configuration dimensions.

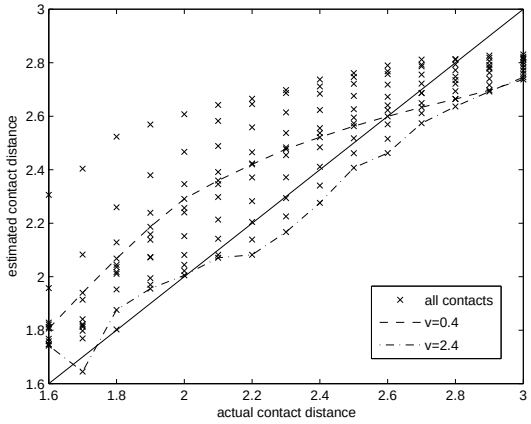

Figure 9. Ground truth (solid line) and estimated (crosses) contact distances d (in cm) under varying velocity (in cm/ms). The minimum and maximum velocities curves are shown (dashed lines). The mean error is 2.0mm.

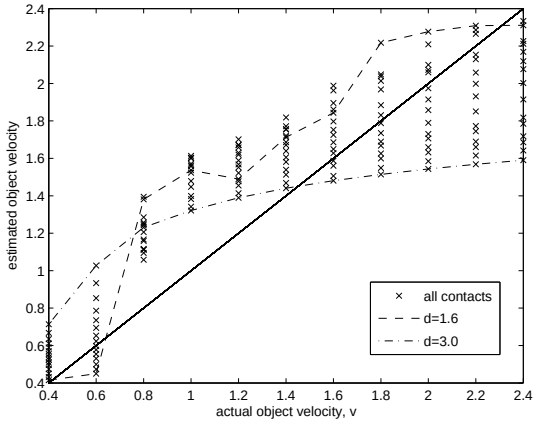

Figure 10. Ground truth (solid line) and estimated (crosses) velocities v (in cm/ms) under varying contact distance. The minimum and maximum contact distance curves are shown (dashed lines). The mean error is 0.28mm/ms.

Many interesting collisions in the real world involve three physical dimensions rather than the 2D collisions produced by simple shapes. For example the act of 'plucking' a whisker (like a musical instrument string) involves pushing the whisker back but simultaneously lifting the object upwards, away from the whisker. Rather than use a full 3D simulation (which massively increases the hidden state space size), a close approximation is to restrict the whisker motion to the horizontal plane while allowing contact object to move in 3D space.

The linear template model demonstrated here is a crude form of discrimination, and more advanced template-based discriminators exist such as classification on Principal and Independent Component strengths. Template models in general are not invariant to shifts

in the time domain, so a different class of Markovian discriminators may be useful instead. These include Hidden Markov Models and recurrent neural networks, which may be trained to filter time-series data into class labels online. Such models have similar dynamic network structure to the full generative model, but are acausal, more easily trainable, and faster to run. In particular, the structural similarity may allow some of their parameters to be set or constrained by knowledge about the generative model.

Previous whiskered shape recognition systems yield only point estimates of contact locations. In contrast generative methods (and discriminative approximations to them) can produce a posterior belief over the configurations of whole objects in the world. These beliefs may then be used as input to higher-level systems. For example localization and mapping tasks [10] and higher-level object recognition from parts [12] are improved by allowing for uncertainty. Uncertainty may be reduced by fusing information from multiple whiskers.

VIII. SUMMARY

Previous approaches to whiskered shape recognition have used only limited subsets of information available from the whiskers. They have further neglected aspects such as the motion, elasticity, and friction of objects. Their outputs have been point estimates of contact points with no posterior distributions, and they have not taken account of uncertainties in sensors or noise in the environment such as wind and self-motion effects.

We have shown how to set up the task as a full generative temporal model, which may in theory account for all available time-series data, and make inferences about the additional object and environment properties. Unusually, the model makes use of an external physics engine to make deterministic state transitions once simple noise terms are drawn. We have shown how the whisker beam can be approximated in this model by a series of masses on springs and discussed some practical simulation issues, in particular noting an empirical trade-off between the computational simulation time and the simulatable stiffness of the whiskers. We propose the use of particle filters for generative inference and for calibrating and testing discriminative methods. Once trained, the latter may in turn suggest new particles to inject into online particle filters.

The utility of full time-series data in recognition was demonstrated by our results showing simultaneous recognition of contact distance and velocity. All previous approaches have assumed static objects. Our result was achieved by a simple template-based discriminator, but suggests that more advanced discriminative and generative models will also be useful and possibly more accurate.

The simulation is available under GPL license from `sourceforge.net/projects/freebots`.

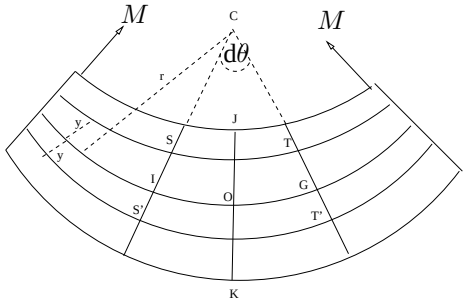

Figure 11. Construction on cross-section of a beam, used to derive the beam theorem.

APPENDIX

Consider fig. 11 which shows the bending. For *pure bending*, the forces rotate with the beam as it bends so they are always perpendicular. The top of the beam experiences negative strain (due to compression stress) and the bottom experiences positive strain (due to tension stress). There will be some 'neutral axis' IOG whose length is unchanged. ST is a short, thin slice at height y from the neutral axis. Consider the strain ϵ_{ST} at ST:

$$\epsilon_{ST} = \frac{\Delta ST}{ST_0} = \frac{ST - IG}{IG} = \frac{(R-y)d\theta - Rd\theta}{Rd\theta} = \frac{-y}{R}.$$

Assuming Hooke's law holds for the stress σ_{ST},

$$\sigma_{ST} = -E\frac{y}{R}.$$

Consider a thin horizontal slice around from ST to $ST + dy$, having cross-sectional area dA, and let the cross-sectional area of the whole beam be A. As there is no axial load, the *total* force horizontally through the beam must be zero (because the beam is static). So

$$F = \int_A \sigma dA = 0$$

(From this it follows by symmetry that the neutral axis is in the center of the beam.) The strain at $S'T'$ is similarly the tensile

$$\epsilon_{s'T'} = \frac{+y}{R}.$$

Imagine that the beam is split into two at JOK. Across ST there is a compressive force

$$F_{ST} = \sigma_{ST} dA = -\frac{Ey}{R} dA$$

acting leftwards on the RHS of the beam and at $S'T'$ there is a similar tensile force $F_{S'T'} = \sigma_{S'T'} dA$ acting rightwards on the RHS of the beam. (And vice versa for the LHS of the beam.) This pair of forces is equivalent to moments about O on the RHS, and the *total* moment on the RHS at location JOK is given by summing them along JOK:

$$M = \int_A y.\frac{Ey}{R} dA = \frac{E}{R}\int_A y^2 dA = \frac{EI}{R}$$

This must be equal to the original bending moment M applied to the RHS and the theorem follows.

IX. REFERENCES

[1] A. Eliazar and R. Parr, "DP-SLAM: Fast, robust simulataneous localization and mapping without predetermined landmarks," in *Proceedings of the Eighteenth International Joint Conference on Artificial Intelligence*, 2003.

[2] M. Kaneko, "Active antenna," in *Fourth IEEE International Conference on Robotics and Automation*, 1994, pp. 2665–2671.

[3] J. Birdwell, J. Solomon, M. Thajchayapong, M. Taylor, M. Cheely, R. Towal, J. Conradt, and M. Hartmann, "Biomechanical models for radial distance determination by the rat vibrissal system." *Journal of Neurophysiology*, vol. 98, no. 4, pp. 2439–55, October 2007.

[4] D. Kim and R. Möller, "Biomimetic whiskers for shape recognition," *Robotics and Autonomous Systems*, vol. 55, no. 3, pp. 229–243, 2007.

[5] G. R. Scholtz and C. D. Rahn, "Profile sensing with an actuated whisker," *IEEE Transactions on Robotics and Automation*, vol. 20, no. 1, pp. 124–127, 2004.

[6] T. Megson, *Structural and Stress Analysis*. Butterworth-Heinemann, 2005.

[7] S. Rao, *Mechanical Vibrations*. Prentice Hall, 2004.

[8] N. Ueno and M. Kaneko, "Dynamic active antenna - a principle of dynamic sensing," in *IEEE ICRA*, 1994, pp. 1784–1790.

[9] C. Fox, M. Pearson, B. Mitchinson, T. Pipe, and T. Prescott, "Simple features for texture classification from robot whisker strains," *Barrels XIX, Atlanta. Abstract in Somatosensory and Motor Research*, vol. 24, no. 3, pp. 139–162, 2007.

[10] S. Thrun, W. Burgard, and D. Fox, *Probabilistic Robotics*. MIT Press, 2005.

[11] C. Fox and J. Quinn, "How to be lost: Principled pruning and priming with particles for score following," in *Proceedings of the International Computer Music Conference*, 2007.

[12] C. Fox, "ThomCat: A Bayesian blackboard model of hierarchical temporal perception," in *Proceedings of the AAAI International FLAIRS Conference*, 2008.